crystals

MDPI

Article

Growth and spectroscopy of Yb:$YMgB_5O_{10}$ crystal

Konstantin N. Gorbachenya[1], Anatol S. Yasukevich[1], Andrey I. Lazarchuk[1], Victor E. Kisel[1], Nikolay V. Kuleshov[1], Elena A. Volkova[2,*], Victor V. Maltsev[2], Elizaveta V. Koporulina[2,3], Vasiliy O. Yapaskurt[4], Nikolai N. Kuzmin[2,5,6], Dmitry A. Ksenofontov[2], Diana D. Mitina[2], Anna I. Jiliaeva[2]

[1] Center for Optical Materials and Technologies, Belarusian National Technical University, Nezalezhnasti Ave., 65, 220013 Minsk, Belarus; lazartschuk1405@gmail.com (A.I.L.); gorby@bntu.by (K.N.G.); anatol@bntu.by (A.S.Y.);vekisel@bntu.by (V.E.K.); nkuleshov@bntu.by (N.V.K.)

[2] Department of Crystallography and Crystal Chemistry, Faculty of Geology, Moscow State University, 119234 Moscow, Russia; volkova@geol.msu.ru (E.A.V.); maltsev@geol.msu.ru (V.V.M.); e_koporulina@mail.ru (E.V.K.); kolyanfclm@mail.ru (N.N.K.); ksen53@gmail.com (D.A.K.); varya-mitya@mail.ru (D.D.M.); annajiliaeva@yandex.ru (A.I.J.)

[3] Melnikov Research Institute of Comprehensive Exploitation of Mineral Resources of the Russian Academy of Sciences, Moscow, Russian Federation; e_koporulina@mail.ru (E.V.K.)

[4] Laboratory of Local Methods for the Study of Matter, Faculty of Geology, Moscow State University, 119234 Moscow, Russia; vyapaskurt@mail.ru (V.O.Y.)

[5] Institute of Spectroscopy of Russian Academy of Science, Fizicheskaya Str. 5, Troitsk, 108840 Moscow, Russia

[6] Moscow Institute of Physics and Technology (National Research University), 9 Institutskiy Per., Dolgoprudny, 141700 Moscow Region, Russia

* Correspondence: volkova@geol.msu.ru

Abstract: A transparent Yb:$YMgB_5O_{10}$ single crystal with dimensions up to 25x23x25 mm and weight of 10.337 g was grown by high-temperature solution growth on dipped seeds technique using $K_2Mo_3O_{10}$ solvent. The Yb^{3+} concentration was calculated to be 4.7 at.% (N_{Yb} = 3.71 × 10^{20} atoms/cm^3) with the distribution coefficient K_d of 0.59. The grown crystal was characterized by means of PXRD, TGA-DSC and ATR-FTIR techniques. The spectral–luminescent properties of the Yb:$YMgB_5O_{10}$ crystal were studied. Absorption cross-section spectra were determined. The luminescence spectra of the Yb:$YMgB_5O_{10}$ crystal are presented in the range of 950–1110 nm. The luminescence kinetics was studied, and the lifetime of the $^2F_{5/2}$ energy level was determined.

Keywords: ytterbium, spectroscopy, rare-earth pentaborate, flux growth, ATR-FTIR spectroscopy.

Citation: Lastname, F.; Lastname, F.; Lastname, F. Title. *Crystals* **2022**, *12*, x. https://doi.org/10.3390/xxxxx

Academic Editor: FirstnameLastname

Received: date
Accepted: date
Published: date

1. Introduction

The presence of high-power laser diodes based on InGaAs compounds in the spectral range of Yb^{3+} absorption (940–980 nm), together with the unique spectroscopic and laser properties of ytterbium-containing materials, stimulated increased interest in the study of new crystalline solids with this activator for various types of lasers emitting near 1 μm. A simple two-level energy scheme of Yb^{3+} ion provides the absence of losses due to absorption from the excited state, up-conversion, cross-relaxation, and other concentration effects, as well as low difference in the energies of pump and generation photons, which ensures significantly lower heat release in the active laser medium, and a wide gain band makes it possible to generate femtosecond pulses [1,2].

Since the first demonstration of a diode-pumped Yb:YAG laser [3], a number of Yb^{3+}-doped crystals have been investigated. Spectroscopic and laser properties of Yb -doped garnets [4–7], tungstates [8–13], vanadates [14–16], aluminates [17–25], phosphates [26–28], sesquioxides [29–31] and borates [32–38] were reported. Tungstate crystals such as Yb:KYW and Yb:KGW have high absorption, the stimulated emission cross sections, and wide emission bands [9, 39], but their thermo-optical properties are

rather low (thermal conductivity is about 3 W/m·K) [40], which limits the use of these crystals in lasers with high average power. Yb-doped sesquioxides (Sc_2O_3, Lu_2O_3, Y_2O_3) exhibit high thermo-optical properties (thermal conductivity up to 12 W/m·K [41, 42]), which makes them attractive active media for high-power lasers. The disadvantages of these crystals are high melting temperatures in the range above 2400°C, difficulties in the production of bulk sesquioxide material of satisfactory quality, small absorption band width (less than 3 nm [41]), and narrow, structured gain spectra [8]. Borate crystals ($Ca_4YO(BO_3)_3$, $Ca_4GdO(BO_3)_3$, $Sr_3Y(BO_3)_3$) with trivalent ytterbium ions Yb^{3+} have wide gain bands and long fluorescence lifetimes of about 2.5 ms, however, these crystals have low absorption and stimulated emission cross sections [8, 27] and low thermal conductivity (~2 W/m·K) [43]. The Yb:$YAl_3(BO_3)_4$ (YAB) crystal combines high absorption and emission cross sections, broad and smooth gain band with the high thermal conductivity (~4.7 W/m·K) [44–48]. Borate crystals $LaMgB_5O_{10}$ also have good thermal conductivity and optical properties [49, 50]. The $YMgB_5O_{10}$ (YMBO) borate crystal is considered as a potential material for manufacturing laser matrices due to its high thermal conductivity (6.2 ± 0.3 W/m·K) and good optical properties [51]. Recently Yb^{3+}-doped YMBO single crystals were grown using K_2O_3–MoO_3 and Li_2O– B_2O_3–LiF fluxes by the top-seeded solution growth method. Their structural, thermal and spectroscopic characteristics were presented [52].

In this paper, the growth and characterization of Yb:$YMgB_5O_{10}$ (YMBO) single crystal, as well as results of its spectroscopic investigation are reported. For the first time ATR-FTIR investigations in the far- and mid-IR ranges have been performed.

2. Materials and Methods

Yb:YMBO bulk crystal was grown by high-temperature solution growth on dipped seeds (HT-SGDS) technique. Based on the previously obtained results [53], a complex system of the composition 20 wt.% Yb:YMBO – 80 wt.% $K_2Mo_3O_{10}$ was used in the growing experiment. Yb_2O_3 (99.96%), Y_2O_3 (99.96%), MgO (A.C.S. grade, produced by Aldrich), B_2O_3 (A.C.S. grade, produced by Alfa Aesar) were used as crystal forming agents, which were weighed according to the composition of $Yb_{0.08}Y_{0.92}MgB_5O_{10}$. The solvent $K_2Mo_3O_{10}$ was a mixture of K_2MoO_4 (A.C.S. grade, Chimkraft, Russia) and MoO_3 (A.C.S. grade, Aldrich production) which was weighed according to the following equation:

$$K_2MoO_4 + 2MoO_3 = K_2Mo_3O_{10}.$$

Growth of Yb:YMBO bulk crystal was performed in a vertical resistively heated furnace, equipped with a Proterm-100 precision temperature controller and a set of S-thermocouples. The temperature in the working zone of the furnace was maintained with stability of ± 0.1°C.

Weighted materials were carefully mixed, grounded, and then the growth charge was loaded into a Pt crucible, heated to 1000°C, and held for 24 hours to assure the homogeneous solution. The choice of solvent composition for single crystal growth experiments was based on previous results on spontaneous synthesis of YMBO crystals from $K_2Mo_3O_{10}$ solvent. Spontaneous YMBO crystals without obvious enclosure and cracking previously obtained from fluxed melt of similar composition were selected and used as seeds for growth experiments (Figure 1).

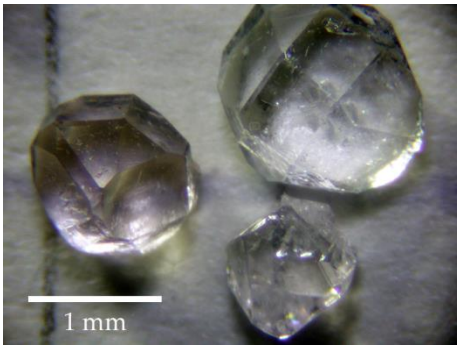

Figure 1. $YMgB_5O_{10}$ spontaneous crystals grown from $K_2Mo_3O_{10}$ - based system.

The saturation temperature of the high-temperature solution was estimated about 880°C by repeated observations of the growth/dissolution trial seed changes upon it contact with the melt surface. The obtained value of saturation temperature for the solute concentration being investigated is in good agreement with the solubility curve of $YMgB_5O_{10}$ in $K_2Mo_3O_{10}$ solvent described by the authors in Ref. [53], and is almost 100 °C lower than that reported in Ref. [52]. During growth, supersaturation was maintained by cooling to 800 °C at a rate from 0.7 to 1.2°C/day and followed by cooling to 300 °C at a rate of 10°/day. Finally, the grown crystal was removed from the furnace, cooled to room temperature for several days to prevent cracking due to heat shock, and then washed in hydrochloric acid.

Powder X-ray diffraction (PXRD) studies were carried out by means of STOE STADI MP powder diffractometer (STOE &Cie GmbH, Germany). PXRD data set was collected in continuous mode at room temperature using CoK_α radiation source (λ = 1.7903 Å) in the range of 2θ = 3–90°. Phase identification was performed using ICSD database [54].

The chemical composition of the Yb:YMBO single crystal was carried out by analytical scanning electron microscope (SEM) technique using JSM-IT-500 (JEOL Ltd., Japan), equipped with the energy-dispersive X-ray (EDX) detector X-Max-n (Oxford Instruments Ltd., GB). SEM was operated at an accelerating voltage of 20 kV and a probe current of 0.7 nA in high-vacuum mode. The sample was coated with a thin layer of carbon for SEM investigations. B_K, Mg_K, Y_L and Yb_L lines in the EDS spectra were used for the elemental composition studies. The distribution coefficient of ytterbium (K_d) was defined as $K_d = C_c / C_d$, where C_c is the Yb content measured in the crystal and C_d is the concentration of Yb in the starting mixture.

Attenuated total reflection (ATR) spectra were measured with a BRUKER IFS 125HR Fourier spectrometer in the spectral range of 50 – 5000 cm^{-1} at room temperature. Measurements were made in the two spectral ranges: in the far IR-range of 50 – 650 cm^{-1} using a Mylar beam-splitter and in the mid-IR range of 400 – 5000 cm^{-1}, with a KBr beam-splitter. In both cases, the Globar was used as the radiation source. DTGS and DLATGS pyroelectric receivers were applied to record interferograms in the far- and mid-IR ranges, respectively.

Differential scanning calorimetry (DSC) and thermogravimetry analysis (TGA) were carried out by means of STA 449 F5 Jupiter® equipment (Netzsch, Germany) in the temperature ranges of 50 – 1500 °C with heating rate of 20 K/min. To clarify the thermal behavior of the investigated compound Yb:YMBO crystals were thermally treated at 1400 °C during 1 hour in muffle furnace PVK -1.6-5 (Russia) equipped with lanthanum chromite-based heater. Products obtained after thermal processing were investigated using PXRD method.

For spectroscopic investigations in polarized light, plates oriented along the three main optical axes of the N_g, N_m, and N_p indicatrices were cut from the Yb:YMBO crystal.

For the polarized absorption spectra measurements, the spectrophotometer CARY 5000 was used. The spectral bandwidth was 0.4 nm.

The absorption cross sections $\sigma_{abs}(\lambda)$ were calculated as follows:

$$\sigma_{abs}(\lambda) = \frac{k_{abs}(\lambda)}{N_{Yb}}, \quad (1)$$

where l is the samples' thickness, N_{Yb} is the ytterbium concentration.

The lifetime measurements were performed using the optical parametric oscillator based on a β-$Ba_2B_2O_4$crystal and pumped by the third harmonic of the Q-switched Nd:YAG laser. The fluorescence from the sample was collected on the entrance slit of the monochromator MDR-12 (LOMO, Russia) and registered by the InGaAs photodiode with preamplifier coupled with a 500 MHz digital oscilloscope.

The luminescence spectrum was recorded in 950-1100 nm spectral range by exciting the crystals with emission of the laser diode at 960 nm. The Yb^{3+} luminescence radiation was dispersed with the MDR-23 monochromator (LOMO, Russia) and detected with the PbS photoresistor supplied with preamplifier connected to the Standford Research Lock-In Amplifier SP830 (Stanford Research Systems, USA).

3. Results and Discussion

3.1. Synthesis, Structure, and Composition

As a result of HT-SGDS experiments transparent, colorless Yb-doped $YMgB_5O_{10}$ crystal with the typically dimensions about 25x23x25 mm and m= 10.337 g was grown (Figure 2).

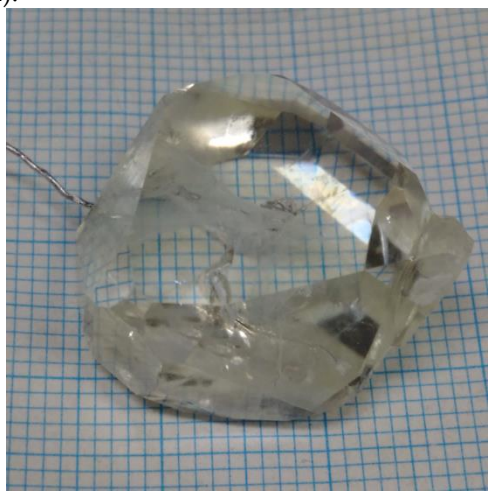

Figure 2. The Yb:$YMgB_5O_{10}$ single crystal grown in 20wt.% Yb:YMBO - 80wt.% $K_2Mo_3O_{10}$ system (1 mm scale).

The PXRD pattern of Yb:YMBO fits well with the one of $YMgB_5O_{10}$ from ICSD database (ICSD #4489) (Figure 3). Element content of Yb:YMBO single crystal was measured at 11 points. The content of each chemical element is in a good agreement with its stoichiometric ratio in the borate formula. From SEM-EDX analysis Yb concentration in the yttrium position was found to be 4.7 at.% with distribution coefficient K_d=0.59. Therefore, the ytterbium concentration N_{Yb} in Yb:YMBO single crystal was calculated to be 3.71 × 10^{20} cm^{-3} using the measured volumetric density of 3.69 g/cm^3 [52].

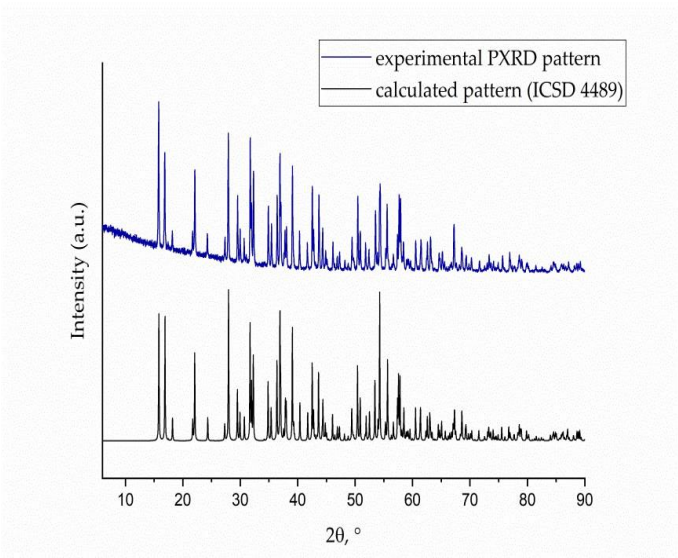

Figure 3. PXRD patterns for Yb:$YMgB_5O_{10}$ (blue) and calculated from *cif*-file for $YMgB_5O_{10}$, ICSD 4489 (black).

According to the structural data from Ref. [55] the unit cell (sp. gr. $P2_1/c$) of $YMgB_5O_{10}$ compound contains N = 68 atoms (Z = 4), which corresponds to $3N$ = 204 degrees of freedom. Three of them are associated with vibrations of the cell as a whole and belong to the acoustic vibrations. Based on these structural data a factor group analysis was carried out. All atoms of the investigated compound Y, Mg, B1 – B5, O1 – O10 are located in the positions C_1. According to the symmetry of the positions of the atoms mentioned above and Ref. [56] each atom generates the following vibrations: $3A_g + 3A_u + 3B_g + 3B_u$. The resulting formula for irreducible representations in the center of the Brillouin zone (Γ_{tot}) consists of acoustic (Γ_{acoust}), optical (Γ_{opt}), Raman active (*Raman*), infrared active (*IR*) modes and has the following form:

$$\Gamma_{tot} = 51A_g + 51A_u + 51B_g + 51B_u \quad (2)$$

$$\Gamma_{acoust} = A_u + 2B_u \quad (3)$$

$$\Gamma_{opt} = 51A_g + 50A_u + 51B_g + 49B_u \quad (4)$$

$$Raman = 51A_g + 51B_g \quad (5)$$

$$IR = 50A_u + 49B_u \quad (6)$$

The ATR-FTIR spectrum of the Yb:YMBO crystal exhibits 37 strong phonons out of 99 expected by factor group analysis (Figure 4). On the one hand, the missing phonons may not be resolved due to the large number of lattice vibrations with close frequencies in this complex compound. This scenario is confirmed by the appearance a flat top in the peaks correlated with phonons near 325, 593, 877 cm^{-1}. On the other hand, absorption below 250 cm^{-1} due to intense phonons is observed. An analysis of the IR active phonon modes was previously conducted in Ref. [55]. According to this work, vibrational modes between 1300 – 1500 cm^{-1} correspond to ν_{as} vibrations of $[BO_3]^{3-}$, ν_{as} vibrations $[BO_4]^{5-}$ there are in the range of 1000 – 1200 cm^{-1}, and ν_s vibrations of $[BO_3]^{3-}$ are observed in the region 800 – 1000 cm^{-1}. However, the authors of the work did not perform a factor group analysis, and IR active phonons below 400 cm^{-1} were not determined.

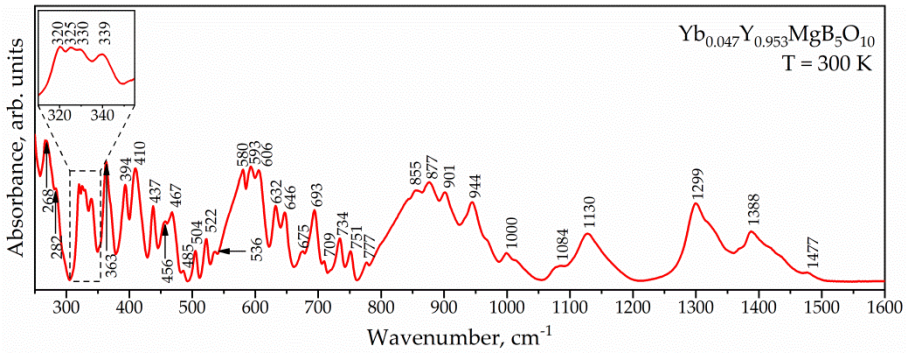

Figure 4. ATR-FTIR spectrum of Yb:YMBO in the range 250 – 1600 cm^{-1} at room temperature.

Data collected during TGA-DSC measurements in the temperature range 50-1500 °C are shown in Figure 5 *a*,*b*. DSC curve exhibit an endothermal peak at ~1051 °C. The absence of an exothermal peak on the cooling curve (insert on Figure 5*a*) and sample appearance suggest a different thermal behavior from that described in [52]. Residue in the crucible after TGA-DSC measurements under heating up to 1150 °C is a white, opaque, dense mass. Repeating heating of the sample in the temperature range of 50-1100 C resulted in a small endothermic peak at ~1047 °C (Figure 5*b*), which may also indicate the decomposition of the studied compound. PXRD analysis revealed the existence of YBO_3 and $Mg_2B_2O_{10}$.

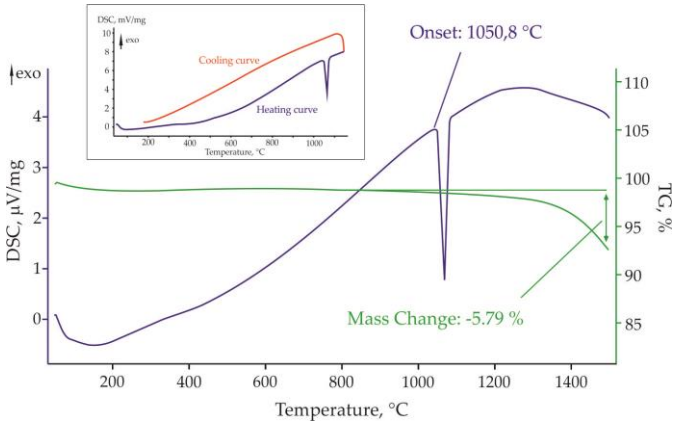

(*a*)

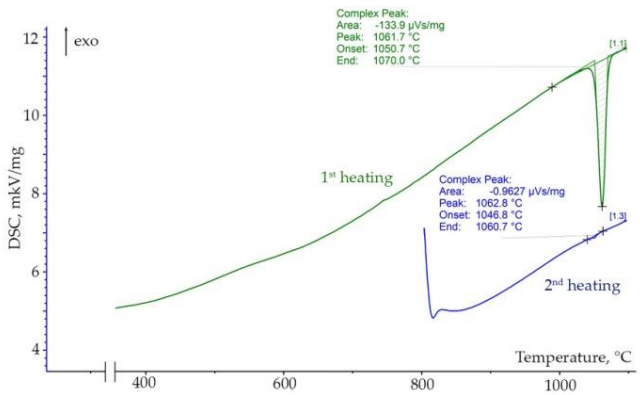

(*b*)

Figure 5. TGA-DSC curves of Yb:YMBO compound: (*a*) data collected in the temperature range of 50-1500 °C and (*b*) repeating heating in the temperature range of 50-1100 °C.

3.2. Spectroscopy

The absorption cross-section spectra of the Yb:YMBO crystal in the spectral range 900–1050 nm are shown in Figure. 6.

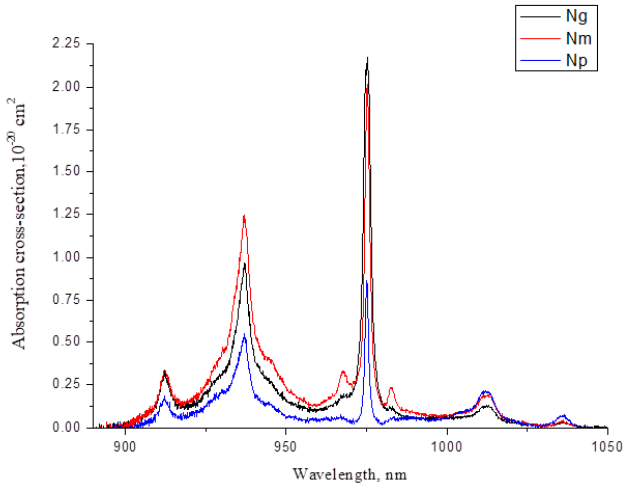

Figure 6. Polarized absorption cross-sectional spectra of Yb^{3+}:YMBO crystal.

Two intensive absorption lines with peaks centered at 937 nm and 975 nm are observed. These peaks coincide with the emission wavelengths of commercially available InGaAs laser diodes. The maximum value of absorption cross-section was determined to be $2.15 \cdot 10^{-20}$ cm^2 at 975 nm with the bandwidth (FWHM) of about 3 nm for polarization E//N_g axis. The narrow absorption band at a wavelength of 975 nm requires thermal stabilization of the pump laser diode. Note, there is a qualitative difference in the peaks' intensities in comparison with previously reported absorption spectra [52].

It is well known that radiation trapping strongly affects the measured luminescence lifetime of Yb-doped materials because of significant overlap of the absorption and emission bands [57,58]. Thus, the special methods discussed in the literature [57, 58] should be used to determine the luminescence lifetime accurately. In our experiments a fine powder of Yb:YMBO crystal immersed in glycerin was used. The dependence of obtained lifetimes of $^2F_{5/2}$ energy level on different weight content of Yb:YMBO crystalline powders in glycerin suspension is presented in Figure 7.

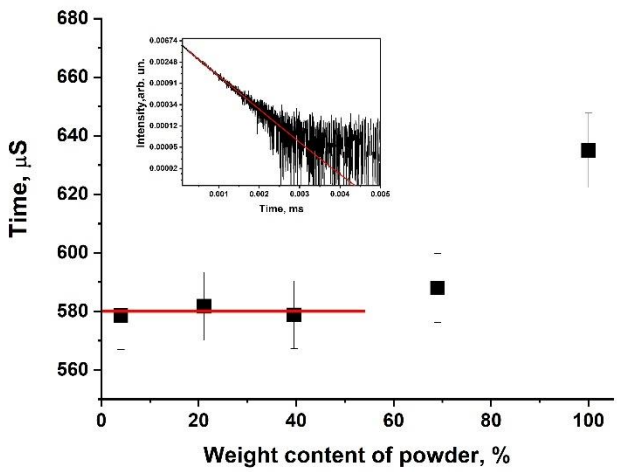

Figure 7. The $^2F_{5/2}$energy level lifetimes of Yb:YMBO crystal.

The decay curve emission was a single exponential one (inset in Figure 7). The fluorescence lifetime decreased with the decreasing of powder concentration in suspension. Starting from a certain powder content, the lifetime remained constant despite further dilution, which indicates negligible reabsorption influence. As a result, the lifetime of $^2F_{5/2}$ energy level was obtained to be about 580 ± 10μs (Figure 7). The obtained luminescence lifetime is shorter compared to one presented in [52] that can be explained by usage technique that enables better elimination of radiation trapping.

Taking into account the radiative lifetime of $^2F_{5/2}$ Yb^{3+} level calculated in [52] the luminescence quantum yield was estimated to be about 0.87. The difference of obtained value from 1 that is a usual case for ytterbium doped materials can be explained by the phonon contribution into deactivation the upper ytterbium level, $^2F_{5/2}$, due to large phonon energy in oxoborate crystals [48].

The polarized luminescence spectra of the Yb:YMBO crystal measured at room temperature are characterized by a structured bands in the spectral range 950–1110 nm (Figure 8) and generally are in a good agreement with results presented in [52]. There are two peaks with maximal intensity at 1010 nm and 1040 nm for E//N_m on the measured luminescence spectrum of Yb:YMBO crystal.

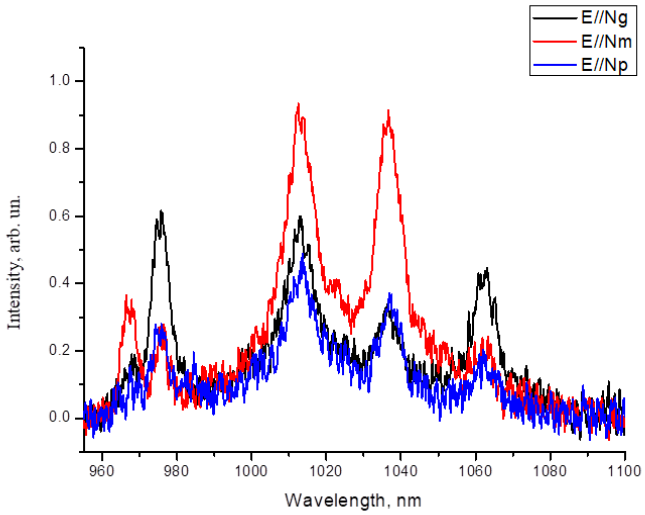

Figure 8. Polarized luminescence spectrum of the Yb:YMBO crystal.

5. Conclusions

Transparent Yb:$YMgB_5O_{10}$ single crystal was grown by high-temperature solution growth on dipped seeds technique using $K_2Mo_3O_{10}$ solvent. The obtained crystal was characterized by means of PXRD, TGA-DSC and ATR-FTIR techniques. The study of the spectral-luminescent properties of the Yb:$YMgB_5O_{10}$ crystal was performed. The usage of obtained crystal for mode-locking and regenerative amplification is the forthcoming prosperity task.

Author Contributions: Writing—original draft preparation, A.I.L., K.N.G., E.A.V.; Formal analysis and investigation, A.I.L., K.N.G., A.S.Y., V.E.K., N.V.K., V.V.M., E.A.V., E.V.K., N.N.K., D.A.K., V.O.Y, D.D.M., A.I.J.; Writing—review and editing, N.V.K., E.A.V. All authors have read and agreed to the published version of the manuscript.

Funding: This research received no external funding.

Conflicts of Interest: The authors declare no conflict of interest.

References

1. Krupke, W.F. Ytterbium solid-state lasers-the first decade. *IEEE J. Quant. Electron***2000**, *6(6)*, 1287–1296.https://doi.org/10.1109/2944.902180.
2. Brunner, F.; Spühler, G.J.; Aus der Au, J.; Krainer, L.; Morier-Genoud, F.; Paschotta, R.; Lichtenstein, N.; Weiss, S.; Harder, C.; Lagatsky, A.A.; Abdolvand, A.; Kuleshov, N.V.; Keller, U. Diode-pumped femtosecondYb:KGd$(WO_4)_2$ laser with 1.1-W average power. *Optics Letters***2000**, *25*, 1119–1121.https://doi.org/10.1364/OL.25.001119.
3. Reinberg, A.R.; Riseberg L.A.; Brown R.M.; Wacker, R.W.; Holton, W.C. GaAs:Si LED pumped Yb-doped YAG laser. *Appl. Phys. Lett.***1971**, *19*, 11-16.https://doi.org/10.1063/1.1653723.
4. Hönninger, C.; Paschotta, R.; Graf, M.; Morier-Genoud, F.; Zhang, G.; Moser, M.;Biswal, S.; Nees, J.; Braun, A.; Mourou, G.A.; Johannsen, I.; Giesen, A.; Seeber, W.; Keller, U. Ultrafast ytterbium-doped bulk lasers and laser amplifiers. *Appl. Phys. B***1999**, *69(1)*, 3–17. https://doi.org/10.1007/s003400050762.
5. Haumesser, P.-H.; Gaumé, R.; Viana, B.; Vivien, D. Determination of laser parameters of ytterbium-doped oxide crystalline materials. *J. Opt. Soc. Am.B***2002**, *19*, 2365–2375.https://doi.org/10.1364/JOSAB.19.002365.
6. Patel, F.D.; Honea, E.C; Speth, J.; Payne, S.A.; Hutcheson, R.; Equall, R. Laser demonstration of $Yb_3Al_5O_{12}$ (YbYAG) and materials properties of highly doped Yb:YAG. *IEEE J. Quant. Electron***2001**, *37*, 135–144.
7. Uemura, S.; Torizuka, K. Sub-40-fs pulses from a diode-pumped kerr-lens modelockedYb-doped yttrium aluminum garnet laser. *Jpn. J. Appl. Phys*. **2011**, *50*, 10201–10203.
8. Brenier, A.; Boulon, G. Overview of the best Yb3+-doped laser crystals, *J. Alloy. Comp*. **2001**, *323*, 210–213. https://doi.org/10.1016/S0925-8388(01)01112-4.
9. Kuleshov, N.V.; Lagatsky, A.A.; Podlipensky, A.V.; Mikhailov, V.P.; Huber, G. Pulsed laser operation of Yb-doped $KY(WO_4)_2$ and $KGd(WO_4)_2$. *Opt. Lett.***1997**, *22*, 1317–1319.https://doi.org/10.1364/OL.22.001317.
10. Demidovich, A.A.; Kuzmin, A.N.; Ryabtsev, G.I.; Danailov, M.B.; Strek, W.; Titov, A.N. Influence of Yb concentration on Yb:KYW laser properties, *J. Alloy. Comp.* **2000**, *300*, 238–241. https://doi.org/10.1016/S0925-8388(99)00777-X.
11. Mateos, X.; Petrov, V.; Aguilo,M.; Sole, R.M.; Gavalda, J.; Massons, J.; Diaz,F.; Griebner, U. Continuous-wave laser oscillation of Yb^{3+} in monoclinic $KLu(WO_4)_2$. *IEEE J. Quant. Electron***2004**, *40*, 1056–1059. https://doi.org/10.1109/JQE.2004.831614.
12. Mateos, X.; Solé, R.; Gavaldà, J.; Aguiló, M.; Massons,J.; Díaz,F.; Petrov,V.; Griebner, U. Crystal growth, spectroscopic studies and laser operation of Yb^{3+}- doped potassium lutetium tungstate. *Opt. Mater.***2006**, *28*, 519–523. https://doi.org/10.1016/j.optmat.2005.01.028.
13. Pujol, M.; Bursukova, M.A.; Güell, F.; Mateos, X.; Solé, R.; Gavaldà, J.; Aguiló, M.; Massons, J.; Díaz, F.; Klopp, P.; Griebner, U.; Petrov, V. Growth, optical characterization, and laser operation of a stoichiometric crystal $KYb(WO_4)_2$. *Phys. Rev. B*,**2002**,*65*,165121–165132.https://doi.org/10.1103/PhysRevB.65.165121.
14. Haumesser, P.-H.; Gaumé, R.; Viana, B.; Antic-Fidancev,E.; Vivien, D. Spectroscopic and crystal-field analysis of new Yb-doped laser materials. *J. Phys. Condens. Matter***2001**, *13*, 5427–5447.https://doi.org/10.1088/0953-8984/13/23/303.
15. Kisel, V.E.; Troshin, A.E.; Tolstik, N.A.; Shcherbitsky, V.G.; Kuleshov, N.V.; Matrosov, V.N.; Matrosova, T.A.; Kupchenko, M.I. Spectroscopy and continuouswave diode-pumped laser action of Yb^{3+}:YVO_4. *Opt. Lett.***2004**, *29*, 2491–2493.https://doi.org/10.1364/OL.29.002491.
16. Sato, Y.; Saikawa, J.; Taira, T.; Nakamura,O.; Furukawa, Y. Spectroscopic properties of Yb:$GdVO_4$ single crystal : Stark levels, selection rules, and polarized cross sections. *Advanced Solid-State Photonics*, Technical Digest Optical Society of America, 2005, MF8.https://doi.org/10.1364/ASSP.2005.MF8.
17. M.J. Weber. Optical properties of Yb^{3+} and Nd^{3+}-Yb^{3+} energy transfer in $YAlO_3$. *Phys. Rev. B***1971**, *4*, 3153–3159.https://doi.org/10.1103/PhysRevB.4.3153.
18. DeLoach, L.D.; Payne, S.A.; Chase, L.L.; Smith, L.K.; Kway, W.L.; Krupke, W.F. Evaluation of absorption and emission properties of Yb^{3+} doped crystals for laser applications.*IEEE J. Quant. Electron.***1993**, *29*, 1179–1191.https://doi.org/10.1109/3.214504.
19. Zeng, X.; Zhao ,G.; Xu,X.; Li, H.; Xu, J.; Zhao, Z.; He, X.; Pang, H.; Jie, M.; Yan, C. Comparison of spectroscopic parameters of 15at% Yb: $YAlO_3$ and 15at% Yb: $Y_3Al_5O_{12}$.*J. Cryst. Growth***2005**, *274*, 106–112.https://doi.org/10.1016/j.jcrysgro.2004.09.086.
20. Zhao, G.; Zeng, X.; Xu, J. Effects of Yb concentration on the fluorescence spectra of Yb-doped $YAlO_3$ single crystals. *Spectrochim. Acta Mol. Biomol. Spectrosc.***2006**, *65* 184–186.https://doi.org/10.1016/J.SAA.2005.10.026.
21. Wang, X.; Xu ,X.; Zhao, Z.; Jiang, B.; Xu, J.; Zhao, G.; Deng, P.; Bourdet, G.; Chanteloup, J.-C. Comparison of fluorescence spectra of Yb:$Y_3Al_5O_{12}$ and Yb:$YAlO_3$ single crystals. *Opt. Mater.* **2007**, 29, 1662–1666.https://doi.org/10.1016/j.optmat.2006.09.01.
22. Eichhorn, M. Quasi-three-level solid-state lasers in the near and mid infrared based on trivalent rare earth ions. *Appl. Phys. B***2008**, *93*, 269–316. https://doi.org/10.1016/ 10.1007/s00340-008-3214-0.
23. Boulon, G.; Guyot, Y.; Canibano, H.; Hraiech S.; Yoshikawa, A. Characterization and comparison of Yb^{3+}-doped $YAlO_3$perovskite crystals (Yb:YAP) with Yb^{3+} -doped $Y_3Al_5O_{12}$ garnet crystals (Yb:YAG) for laser application, *J. Opt. Soc. Am. B***2008**, *25*, 884–896.https://doi.org/10.1364/JOSAB.25.000884.

24. Petit, P.O.; Goldner, P.; Viana, B.;Boudeile, J.; Didierjean, J.; Balembois, F.; Druon, F.; Georges, P. Diode pumping of Yb^{3+}:$CaGdAlO_4$, Proceedings Of International Conference on Lasers, Applications, and Technologies: Solid State Lasers and Amplifiers III, Strasburg, France 2008, 6998,1–6.
25. Li, D.; Xu, X.; Cheng, Y.; Cheng, S.; Zhou, D.; Wu, F.; Xia, C.; Xu, J.; Zhang, J. Crystal growth and spectroscopic properties of Yb:$CaYAlO_4$ single crystal. *J. Cryst. Growth***2010**, *312*, 2117–2121.https://doi.org/10.1016/j.jcrysgro.2010.04.028.
26. Brenier, A. A new evaluation of Yb^{3+}-doped crystals for laser applications.*J. Lumin.***2001**, 199-204.https://doi.org/10.1016/S0022-2313(00)00258-1.
27. Bayramian, A.J.; Bibeau, C.; Beach, R.J.; Marshall, C.D.; Payne, S.A.; Krupke, W.F. Three-level Q-switched laser operation of ytterbium-doped $Sr_5(PO_4)_3F$ at 985 nm. *Opt. Lett.* **2000**, *25*, 622–624.https://doi.org/10.1364/OL.25.000622.
28. Schaffers, K.I.; Tassano, J.B.; Bayramian, A.B.; Morris, R.C. Growth of Yb: S-FAP [Yb^{3+}: $Sr_5(PO_4)_3F$] crystals for the Mercury laser. *J. Cryst. Growth***2003**, *253*, 297–306. https://doi.org/10.1016/S0022-0248(03)01032-7.
29. Petermann, K.; Huber,G.;Fornasiero, L.; Kuch, S.; Mix, E.; Peters, V.; Basun, S.A. Rareearth-doped sesquioxides. *J. Lumin.***2000**, *89*, 973–975.https://doi.org/10.1016/S0022-2313(99)00497-4.
30. Peters, V. Growth and Spectroscopy of Ytterbium-Doped Sesquioxides. Ph.D. Thesis, Hamburg, Germany, 2001.
31. Brenier, A.; Boulon, G. New criteria to choose the best Yb^{3+}-doped laser crystals, *Europhys. Lett.***2001**, *55*, 647–652. •https://doi.org/10.1209/EPL/I2001-00465-1.
32. Chénais, S.; Druon, F.; Balembois, F.; Georges, P.; Gaumé, R.; Haumesser, P.H.; Viana, B.; Aka, G.P.; Vivien, D. Spectroscopy and efficient laser action from diode pumping of a new broadly tunable crystal: Yb^{3+}:$Sr_3Y(BO_3)_3$. *J. Opt. Soc. Am.B***2002**, *19*, 1083–1091. https://doi.org/10.1364/JOSAB.19.001083.
33. Földvári, I.; Beregi, E.; Baraldi, A.; Capelletti, R.; Ryba-Romanowski, W.; Dominiak Dzik, G.; Munoz, A.; Sosa, R. Growth and spectroscopic properties of rare-earth doped $YAl_3(BO_3)_4$ single crystals. *J. Lumin.***2003**, *102*, 395–401. https://doi.org/10.1016/S0022-2313(02)00533-1.
34. Wang, P.; Dawes, J.M.; Dekker, P.; Piper, J.A. Spectral properties and infrared laser performance of diode-pumped Yb:$YAl_3(BO_3)_4$. *Opt. Soc. Am.***1999**, *26*, 614-617.
35. Liu, J.; Mateos, X.; Zhang, H.; Li, J.; Wang, J.;Petrov, V. High-power laser performance of Yb:$YAl_3(BO_3)_4$ crystals cut along the crystallographic axes. *IEEE J. Quant. Electron*. **2007**, *43*, 385–390.
36. Aron, A.; Aka, G.; Viana, B.; Kahn-Harari, A.; Vivien, D.; Druon, F.; Balembois, F.; Georges, P.; Brun, A.; Lenain, N.; Jacquet, M. Spectroscopic properties and laser performances of Yb:YCOB and potential of the Yb:LaCOB material. *Opt. Mater.***2001**, *16*, 181–188. https://doi.org/10.1016/S0925-3467(00)00075-6.
37. Wang, P.; Dawes, J.M.; Dekker, P.; Zhang ,H.;Meng, X. Spectral characterization and diode-pumped laser performance of Yb:YCOB. *Opt. Soc. Am.***1999**, *26*, 631-634. https://doi.org/10.1364/ASSL.1999.ME14.
38. Druon, F.; Chénais, S.; Balembois, F.; Georges, P.; Brun, A.; Courjaud, A.; Hönninger, C.; Salin, F.; Zavelani-Rossi, M.; Augé, F.; Chambaret, J.P.; Aron, A.; Mougel, F.; Aka, G.; Vivien, D. High-power diode-pumped Yb:GdCOB laser: from continuous-wave to femtosecond regime. *Opt. Mater.***2002**, *19*, 73-80. https://doi.org/10.1016/S0925-3467(01)00203-8.
39. Kuleshov, N.V.; Lagatsky, A.A.; Shcherbitsky, V.G.; Mikhailov, V.P.; Heumann, E.; Jensen, T.; Diening, A.; Huber, G. CW laser performance of Yb and Er,Yb doped tungstates. *J. Appl. Phys. B*, **1997**, *64*,409-413. https://doi.org/10.1007/S003400050191.
40. Aggarwal, R.L.; Ripin, D.J.; Ochoa, J.R.; Fan, T.Y. Measurement of thermo-optic properties of $Y_3Al_5O_{12}$, $Lu_3Al_5O_{12}$, $YAlO_3$, $LiYF_4$, $LiLuF_4$, BaY_2F_8,$KGd(WO_4)_2$, and $KY(WO_4)_2$ laser crystalsin the 80-300 K temperature range. *J. Appl. Phys. B***2005**, *98*, 103514.https://doi.org/10.1063/1.2128696.
41. Peters, R.; Kränkel, C.; Fredrich-Thornton, S.T.; Beil, K.; Petermann, K.; Huber, G.; Heckl, O.H.; Baer, C.R.E.; Saraceno, C.J.; Südmeyer, T.; Keller,U. Thermal analysis and efficient high power continuous-wave and mode-locked thin disk laser operation of Yb-doped sesquioxides. *J. Appl. Phys. B.***2011**, *102*, 509-514.https://doi.org/10.1007/s00340-011-4428-0.
42. Mun, J.H.; Jouini, A.; Yoshikawa, A.; Kim, J.-H.; Fukuda, T.; Lee, J. Thermal and optical properties of Yb-doped Lu_2O_3 single crystal grown by the micro-pulling-down method. *J. Ceramic Process***2013**, *14*, 636-640.
43. Mougel, F.; Kahn-Harari, A.; Aka, G.; Pelenc, D. Structural and thermal stability of Czochralski grown GdCOBoxoborate single crystals. *J. Mater. Chem.***1998**, *8*, 1619–1623.https://doi.org/10.1039/A800492G.
44. Blows, J.L.; Dekker, P.; Wang, P.; Dawes, J.M.; Omatsu, T. Thermal lensing measurements and thermal conductivity of Yb:YAB. *Appl. Phys. B***2003**, *76*, 289–292. https://doi.org/10.1007/s00340-002-1092-4.
45. Wang, P.; Dawes, J.M.; Dekker, P.; Knowles, D.S.; Piper, A.J. Lu, BGrowth and evaluation of ytterbium-doped yttrium aluminum borate as a potential self-doubling laser crystal.*J. Opt. Soc. Am. B***1999**, *16*, 63–69.https://doi.org/10.1364/JOSAB.16.000063.
46. Liao, J.; Lin, Y.; Chen, Y.; Luo, Z.; Huang, Y. Flux growth and spectral properties of Yb:YAB single crystal with high Yb^{3+} concentration. *J. Cryst. Growth***2004**, *267*, 134–139. https://doi.org/10.1016/j.jcrysgro.2004.03.026.
47. Wang, P.; Dawes, J.M.; Dekker, P.; Piper, J.A. Highly efficient diode-pumped ytterbium-doped yttrium aluminum borate laser. *Opt.Commun.***2000**, *174*, 467–470. https://doi.org/10.1016/S0030-4018(99)00686-0.
48. Rudenkov A.S.; Kisel V.E.; Gorbachenya K.N.; Yasukevich A.S.; Maltsev V.V.; Leonyuk N.I.; Rubtsova N.N.; Semyagin B.R.; Kovalyov A.A.; V.V. Preobrazhenskii; Kuleshov N.V. Growth, spectroscopy and high power laser operation of Yb:$YAl_3(BO_3)_4$

crystal: continuous-wave, mode-locking and chirped pulse regenerative amplification. *Optical Materials* **2019**, 89, 261-267. https://doi.org/ 10.3390/cryst12040519.

49. Huang, Y.S.; Zhou, W.W.; Sun, S.J.; Yuan, F.F.; Zhang, L.Z.; Zhao, W.; Wang, G.F.; Lin, Z.B. Growth, structure, spectral and laser properties of Yb^{3+}:$LaMgB_5O_{10}$ – a new laser material. *CrystEngComm* **2015**, *17*, 7392. https://doi.org/10.1039/C5CE01443C.
50. Huang, Y.S.; Chen, H.B.; Sun, S.J.; Yuan, F.F.; Zhang, L.Z.; Lin, Z.B.; Zhang, G.; Wang, G.F. Growth, thermal, spectral and laser properties of Nd^{3+}:$LaMgB_5O_{10}$ crystal - a new promising laser material.*J. Alloy. Compd.* **2015***646*, 1083-1088. https://doi.org/10.1016/j.jallcom.2015.06.196.
51. Mitina, D.D.; Maltsev, V.V.; Leonyuk, N.I.; Gorbachenya, K.N.; Deineka, R.V.; Kisel, V.E.; Yasukevich, A.S.; Kuleshov, N.V. Growth and characterization of *R*MgB_5O_{10} (R=Y, La, Gd) crystals. *Inorg. Mater.* **2020**, *56*, 211-222. https://doi.org/10.1134/S0020168520020132.
52. Sun, S.; Li, B.; Lou, F.; Shi, X.; Chen, W.; Yuan, F.; Zhang, L.; Lin, Z.; Zhong, D.; Huang, Y.; Teng, B. Optimization of fluxes for Yb^{3+}:$YMgB_5O_{10}$ crystal growth and intense multi-wavelength emission characteristics in spectral and laser performances. *J. Mater. Chem.* **2021**, *9*, 14766. https://doi.org/10.1039/d1tc03909a.
53. Maltsev, V.V.; Mitina D.D.; Belokoneva E.L.; Volkova E.A.; Koporulina E.V.; Jiliaeva A.I. Synthesis and flux growth of rare-earth magnesium pentaborate crystals $RMgB_5O_{10}$ (R=Y, Gd, La, Tm and Yb). *J.Cryst. Growth***2022**, *587*, 126628. https://doi.org/10.1016/j.jcrysgro.2022.126628.
54. Inorganic Crystal Structure Data Base – ICSD; Fachinformationzentrum (FIZ) Karlsruhe: Karlsruhe, Germany, 2021.
55. Zhang, J.; Tao, X.; Cai, G.; Jin, Z. Phase relation, structure, and properties of borate $MgYB_5O_{10}$ in $MgO–Y_2O_3–B_2O_3$ system. *Powder diffraction* **2017**, *32*, 97-106. https://doi.org/10.1017/S0885715617000227.
56. Rousseau, D.L.; Bauman, R.P.; Porto, S.P.S. Normal mode determination in crystals. *J. Raman Spectroscopy* **1981**, *10*, 253-290. https://doi.org/10.1002/JRS.1250100152.
57. Sumida, D.S.; Fan, T.Y. Effect of radiation trapping on fluorescence lifetime and emission cross section measurements in solid-state laser media . *Opt. Lett*. **1994**, *19*, 1343-1345. https://doi.org/10.1364/OL.19.001343.
58. Kühn, H.; Fredrich-Thornton, S.T.; Kränkel, C.; Peters, R.; Petermann, K. Model for the calculation of radiation trapping and description of the pinhole method. *Opt. Lett.***2007**, *32*, 1908-1910. https://doi.org/10.1364/OL.32.001908.